Synthesis and Properties of Linear-Type S-Bridged $Rh^{III}Ni^{II}Rh^{III}$ Trinuclear Complexes with 2-Aminoethanethiolate (aet) or L-Cysteinate (L-cys). Crystal Structure of $[Ni\{Rh(aet)_3\}_2](NO_3)_2$

Takumi Konno* and Ken-ichi Okamoto

Department of Chemistry, University of Tsukuba, Tsukuba, Ibaraki 305

(Received September 5, 1994)

The reaction of *fac*(*S*)-[Rh(aet)$_3$] with Ni^{2+} at room temperature gave a linear-type S-bridged $Rh^{III}Ni^{II}Rh^{III}$ trinuclear complex, $[Ni\{Rh(aet)_3\}_2]^{2+}$ (**1**). A similar reaction of Δ_{LLL}-*fac*(*S*)-[Rh(L-cys-*N*,*S*)$_3$]$^{3-}$ with Ni^{2+} produced the corresponding trinuclear complex with L-cys ligands, $\Delta_{LLL}\Delta_{LLL}$-$[Ni\{Rh(L\text{-cys-}N,S)_3\}_2]^{4-}$ ($\Delta_{LLL}\Delta_{LLL}$-**2**), retaining the Δ_{LLL} configuration of the starting complex. The crystal structure of **1**$(NO_3)_2$ was determined by X-ray diffraction. $[Ni\{Rh(aet)_3\}_2](NO_3)_2\cdot 2H_2O$, chemical formula $C_{12}H_{40}N_8S_6O_8NiRh_2$, crystallizes in the triclinic space group $P\bar{1}$ with a=12.249(3), b=13.366(4), c=10.260(2) Å, α=108.76(1), β=102.46(1), γ=101.21(1)°, V=1488.7(7) Å^3, Z=2, and R=0.024. In **1** the central Ni^{II} atom is situated in a distorted octahedral geometry, coordinated by six thiolato sulfur atoms from the two octahedral *fac*(*S*)-[Rh(aet)$_3$] units. The two *fac*(*S*)-[Rh(aet)$_3$] units have the same absolute configuration to form the racemic ($\Delta\Delta/\Lambda\Lambda$) isomer. The optically active $\Delta\Delta$ and $\Lambda\Lambda$ isomers of **1** were derived from $\Delta\Delta\Delta\Delta$- and $\Lambda\Lambda\Lambda\Lambda$-$[\{Rh(aet)_3\}_4Zn_3(HO)]^{5+}$ respectively, by adding excess Ni^{2+}. The electronic absorption spectral behavior of **1** indicated that the intermolecular exchange of the *fac*(*S*)-[Rh(aet)$_3$] units occurs in solution, which results in the formation of the $\Delta\Lambda$ (*meso*) isomer from a 1 : 1 mixture of the $\Delta\Delta$ and $\Lambda\Lambda$ isomers. The chemical properties of the present $Rh^{III}Ni^{II}Rh^{III}$ complexes are discussed in comparison with those of the corresponding $Co^{III}Ni^{II}Co^{III}$ and $Rh^{III}Co^{III}Rh^{III}$ complexes.

It has been recognized that the mononuclear *fac*(*S*)-[M(aet)$_3$] and *fac*(*S*)-[M(L-cys-*N*,*S*)$_3$]$^{3-}$ complexes (M=Co^{III}, Rh^{III}, Ir^{III}; aet=$NH_2CH_2CH_2S^-$; L-cys=$NH_2CH(COO^-)CH_2S^-$) readily react with a variety of metal ions to form S-bridged polynuclear complexes.[1—24] For example, the reactions of *fac*(*S*)-[M(aet or L-cys-*N*,*S*)$_3$]$^{0\text{ or }3-}$ with octahedral Co^{III} give linear-type S-bridged trinuclear complexes, $[Co^{III}\{M(aet\text{ or L-cys-}N,S)_3\}_2]^{3+\text{ or }3-}$,[1—10] while the reactions with tetrahedral Zn^{II} produce T-cage-type S-bridged octanuclear complexes, $[\{M(aet\text{ or L-cys-}N,S)_3\}_4Zn_4O]^{6+\text{ or }6-}$.[17—21] For the reaction products of *fac*(*S*)-[Co(aet or L-cys-*N*,*S*)$_3$]$^{0\text{ or }3-}$ and Ni^{II}, which possibly takes a tetrahedral or square-planar geometry besides an octahedral one, a linear-type S-bridged $Co^{III}Ni^{II}Co^{III}$ trinuclear structure, $[Ni\{Co(aet\text{ or L-cys-}N,S)_3\}_2]^{2+\text{ or }4-}$, has been proposed based mainly on the spectral and magnetic properties,[1,6] and this structure has recently been confirmed by the X-ray analysis for $[Ni\{Co(aet)_3\}_2]^{2+}$.[15] Though the crystal structure of $[Ni\{Co(aet)_3\}_2]^{2+}$ is very similar to that of $[Co\{Co(aet)_3\}_2]^{3+}$,[3,15] it has been pointed out that the electronic absorption and CD spectral features of $[Ni\{Co(aet\text{ or L-cys-}N,S)_3\}_2]^{2+\text{ or }4-}$ differ from those of $[Co\{Co(aet\text{ or L-cys-}N,S)_3\}_2]^{3+\text{ or }3-}$ especially in the visible region.[6] In addition, only the racemic ($\Delta\Delta/\Lambda\Lambda$) isomer has been obtained for $[Ni\{Co(aet)_3\}_2]^{2+}$,[1,15] while $[Co\{Co(aet)_3\}_2]^{3+}$ gave all three possible isomers, $\Delta\Delta$, $\Lambda\Lambda$, and $\Delta\Lambda$.[2,7] In this paper, we report on the synthesis, structure, and chemical properties of novel linear-type S-bridged $Rh^{III}Ni^{II}Rh^{III}$ complexes, $[Ni\{Rh(aet\text{ or L-cys-}N,S)_3\}_2]^{2+\text{ or }4-}$, which afford a clearer understanding of the spectrochemical and stereochemical differences between the S-bridged trinuclear complexes with Ni^{II} and those with Co^{III} at the center of the structure.

Experimental

Preparation of Complexes. $Ni\{Rh(aet)_3\}_2](NO_3)_2$ (1$(NO_3)_2$). To a suspension containing 0.10 g (0.30 mmol) of *fac*(*S*)-[Rh(aet)$_3$][20,25] in 10 cm^3 of water was added 0.10 g (0.34 mmol) of $Ni(NO_3)_2\cdot 6H_2O$. The mixture was stirred at room temperature for 20 min and the resulting red crystalline product was collected by filtration. This product was dissolved in a small amount of hot water (about 60 °C) and left at room temperature overnight. The resulting fine red crystals (**1**$(NO_3)_2\cdot 2H_2O$) were collected by filtration and washed with a small amount of ethanol. Single crystals suitable for X-ray analysis were obtained by recrystallization of the fine red crystals from water at room temperature. Yield: 0.09 g (68%). Anal. Found: C, 16.40;

H, 4.68; N, 12.70; Ni, 6.31; Rh, 22.90%. Calcd for $[Ni\{Rh(C_2H_6NS)_3\}_2](NO_3)_2\cdot 2H_2O$: C, 16.35; H, 4.57; N, 12.71; Ni, 6.66; Rh, 23.35%.

The chloride and bromide salts of **1** were prepared by the same method used for the nitrate salt, using $NiCl_2\cdot 6H_2O$ and $NiBr_2$ instead of $Ni(NO_3)_2\cdot 6H_2O$. All the complex salts showed the same absorption spectra. Yield for the chloride salt: 0.08 g (63%). Yield for the bromide salt: 0.11 g (79%). Anal. Found for the chloride salt: C, 17.14; H, 5.14; N, 9.93%. Calcd for $[Ni\{Rh(C_2H_6NS)_3\}_2]Cl_2\cdot 3.5H_2O$: C, 17.13; H, 5.00; N, 9.93%. Found for the bromide salt: C, 15.78; H, 4.50; N, 9.10%. Calcd for $[Ni\{Rh(C_2H_6NS)_3\}_2]Br_2\cdot 2H_2O$: C, 15.71; H, 4.40; N, 9.16%.

$(+)^{CD}_{420}$-$\Delta\Delta$- and $(-)^{CD}_{420}$-$\Lambda\Lambda$-$[Ni\{Rh(aet)_3\}_2](NO_3)_2$ ($\Delta\Delta$- and $\Lambda\Lambda$-1$(NO_3)_2$). To a solution containing 0.15 g (0.08 mmol) of $\Delta\Delta\Delta\Delta$- or $\Lambda\Lambda\Lambda\Lambda$-$[\{Rh(aet)_3\}_4Zn_3(HO)](NO_3)_5\cdot 2H_2O$[19] in 5 cm^3 of water was added 0.20 g (0.69 mmol) of $Ni(NO_3)_2\cdot 6H_2O$. The mixture was stirred at 40 °C for 30 min, during which time the solution color turned from orange-yellow to dark red and fine red crystals began to appear. After the reaction mixture was left at room temperature for 3 h, the resulting fine crystals were collected by filtration. Yield for both the $(+)^{CD}_{420}$ and $(-)^{CD}_{420}$ isomers: 0.03 g (21%). Anal. Found for the $(-)^{CD}_{420}$ isomer: C, 16.41; H, 4.64; N, 12.63; Ni, 6.36; Rh, 22.96%. Found for the $(+)^{CD}_{420}$ isomer: C, 16.26; H, 4.57; N, 12.61%. Calcd for $[Ni\{Rh(C_2H_6NS)_3\}_2](NO_3)_2\cdot 2H_2O$: C, 16.35; H, 4.57; N, 12.71; Ni, 6.66; Rh, 23.35%.

$(+)^{CD}_{420}$-$\Delta_{LLL}\Delta_{LLL}$-$Na_4[Ni\{Rh(L\text{-}cys\text{-}N,S)_3\}_2]$ ($\Delta_{LLL}\Delta_{LLL}$-$Na_4$2). A 0.1 g (0.22 mmol) sample of Δ_{LLL}-*fac*(*S*)-$H_3[Rh(L\text{-}cys\text{-}N,S)_3]$[9,20] was dissolved in 5 cm^3 of water by adding 1.0 mol dm^{-3} NaOH. To this yellow solution (about pH=8) was added 0.06 g (0.25 mmol) of $NiCl_2\cdot 6H_2O$. The solution color immediately turned to dark red. After the mixture was stirred at room temperature for 10 min, a large amount of ethanol was added to it in an ice bath. The resulting dark orange powder was collected by filtration and recrystallized from water by adding ethanol in an ice bath. Yield: 0.09 g (63%). Anal. Found: C, 16.56; H, 4.22; N, 6.36%. Calcd for $Na_4[Ni\{Rh(C_2H_5O_2NS)_3\}_2]\cdot 13H_2O$: C, 16.56; H, 4.32; N, 6.44%.

Measurements. The electronic absorption spectra were recorded with a JASCO Ubest-55 or UVIDEC-505 spectrophotometer, and the CD spectra with a JASCO J-600 spectropolarimeter. The elemental analyses (C, H, N) were done by the Analysis Center of the University of Tsukuba. The concentrations of Ni and Rh in the representative complexes were measured with a Nippon Jarrel-Ash ICPA-575 ICP spectrophotometer.

X-Ray Structure Analysis. A red crystal (about 0.15×0.12×0.08 mm) of **1**$(NO_3)_2$ was used for data collection on an Enraf–Nonius CAD4 diffractometer with a graphite-monochromatized Mo $K\alpha$ radiation ($\lambda=0.71073$ Å). Unit cell dimensions were determined by least-squares refinement of 25 reflections with $15°<2\theta<20°$. Crystal data: $[Ni\{Rh(aet)_3\}_2](NO_3)_2\cdot 2H_2O=C_{12}H_{40}N_8S_6O_8NiRh_2$, $M=881.4$, triclinic, space group $P\bar{1}$ (No. 2), $a=12.249(3)$, $b=13.367(4)$, $c=10.260(2)$ Å, $\alpha=108.76(1)$, $\beta=102.46(1)$, $\gamma=101.21(1)°$, $V=1488.7(7)$ Å^3, $Z=2$, $D_c=1.97$ g cm^{-3}, $F(000)=892$, μ (Mo $K\alpha$)=21.6 cm^{-1}, and room temperature.

The intensity data were collected by the ω–2θ scan mode up to $2\theta=50°$ ($-14\leqq h\leqq 14$, $-15\leqq k\leqq 15$, $0\leqq l\leqq 12$) with scan width $(1.20+0.35\tan\theta)°$ and scan rate varied from 1 to 5° min^{-1} (on ω). The intensities were corrected for Lorentz and polarization. An empirical absorption correction based on a series of ψ scans was applied (max and min transmission factors, 1.00 and 0.87). A total of 4356 independent reflections with $I>3\sigma(I)$ of the measured 5546 reflections were considered as 'observed' and used for the structure determination.

The structure was solved by a direct method and difference Fourier techniques and refined by full-matrix least squares using anisotropic thermal parameters for non-hydrogen atoms.[26] Hydrogen atoms were located and their positions and isotropic thermal parameters were refined. The final refinement gave $R=0.024$ and $R_w=0.026$ $[w=4F_o^2/\sigma^2(F_o)^2]$. Non-hydrogen atom coordinates for the complex cation are listed in Table 1.[27]

Table 1. Final Atomic Coordinates and Equivalent Isotropic Thermal Parameters (B_{eq}/Å^2) for Non-Hydrogen Atoms of **1**$(NO_3)_2\cdot 2H_2O$

Atom	x	y	z	B_{eq}[a]
Ni	0.21803(4)	0.48413(4)	0.27729(5)	2.07(1)
Rh1	0.16532(3)	0.26743(2)	0.04499(3)	1.889(6)
Rh2	0.27453(2)	0.69549(2)	0.52189(3)	1.862(6)
S1	0.19727(9)	0.43764(7)	0.0229(1)	2.39(2)
S2	0.04735(8)	0.32386(8)	0.1871(1)	2.23(2)
S3	0.32367(8)	0.34614(7)	0.2535(1)	2.28(2)
S4	0.21336(8)	0.52027(7)	0.5221(1)	2.27(2)
S5	0.39964(8)	0.63580(8)	0.3927(1)	2.38(2)
S6	0.13241(8)	0.63442(7)	0.30157(9)	2.21(2)
N1	0.2768(3)	0.2333(3)	−0.0850(4)	3.07(8)
N2	0.0108(3)	0.2006(3)	−0.1314(3)	2.72(8)
N3	0.1504(3)	0.1210(3)	0.0876(3)	2.67(8)
N4	0.4025(3)	0.7306(3)	0.7209(4)	2.88(8)
N5	0.3382(3)	0.8496(3)	0.5084(4)	2.90(8)
N6	0.1440(3)	0.7395(3)	0.6149(3)	2.82(8)
C1	0.3347(4)	0.4353(4)	−0.0173(5)	3.4(1)
C2	0.3186(4)	0.3237(4)	−0.1317(5)	4.0(1)
C3	−0.0748(4)	0.3096(3)	0.0379(4)	2.96(9)
C4	−0.0945(4)	0.2016(3)	−0.0834(4)	3.0(1)
C5	0.2788(4)	0.2437(3)	0.3287(4)	2.84(9)
C6	0.2472(4)	0.1309(3)	0.2116(5)	3.2(1)
C7	0.3480(4)	0.5306(3)	0.6496(4)	3.00(9)
C8	0.3832(4)	0.6393(4)	0.7740(4)	3.2(1)
C9	0.4064(4)	0.7408(3)	0.3147(4)	3.3(1)
C10	0.4280(4)	0.8520(3)	0.4336(5)	3.7(1)
C11	0.0099(3)	0.6235(3)	0.3750(4)	2.82(9)
C12	0.0349(4)	0.7267(3)	0.5063(4)	3.08(9)
N1n	0.4670(3)	0.9193(3)	0.1095(4)	3.50(9)
N2n	0.1710(4)	0.0384(3)	0.5354(4)	3.9(1)
O11	0.3661(4)	0.8604(4)	0.0505(5)	7.4(1)
O12	0.4905(5)	1.0131(4)	0.1905(5)	8.1(2)
O13	0.5400(4)	0.8796(4)	0.0752(8)	10.5(2)
O21	0.2141(4)	0.0237(3)	0.6460(4)	6.9(1)
O22	0.1669(4)	−0.0287(3)	0.4176(4)	5.3(1)
O23	0.1280(4)	0.1143(3)	0.5417(5)	6.8(1)
O1w	−0.0118(3)	0.0393(2)	0.2368(3)	3.68(8)
O2w	0.2491(3)	0.9528(3)	0.8822(4)	4.54(9)

a) B_{eq} is the arithmetic mean of the principal axes of the thermal ellipsoid.

Results and Discussion

Crystal Structure of $[Ni\{Rh(aet)_3\}_2](NO_3)_2$ ($1(NO_3)_2$). X-Ray structural analysis revealed the presence of a discrete complex cation, two nitrate anions, and two water molecules. A perspective drawing of the complex cation is given in Fig. 1 and its selected bond lengths and angles are listed in Table 2.

The complex cation consists of two approximately octahedral *fac*(*S*)-[Rh(aet)$_3$] units and one nickel atom. This is consistent with the plasma emission spectral analysis, which gave a value of Ni:Rh=1:2. The three thiolato sulfur atoms in each *fac*(*S*)-[Rh(aet)$_3$] unit coordinate to the central nickel atom, forming a linear-type S-bridged $Rh^{III}Ni^{II}Rh^{III}$ trinuclear structure (Rh1–Ni–Rh2=176.76(2)°, Ni–Rh1=2.9423(5) Å, Ni–Rh2=2.9478(5) Å). The coordination geometry of the central nickel atom is distorted from a regular octahedron, having acute S–Ni–S bite angles (average 83.26(4)°). In the terminal *fac*(*S*)-[Rh(aet)$_3$] units, the S–Rh–S angles (average 88.03(4)°) are close to right angles, while the N–Rh–N angles (average 95.1(2)°) are significantly deviated from 90° to give the expanded N_3 faces.

The overall structure of **1** is similar to that of the corresponding linear-type $Co^{III}Ni^{II}Co^{III}$ complex, $[Ni\{Co(aet)_3\}_2]^{2+}$.[15] In particular, the bond angles around the central nickel and the terminal rhodium atoms in **1** are quite similar to those around the central nickel (average S–Ni–S=81.26(3)°) and the terminal cobalt atoms (average S–Co–S=87.88(4)° and N–Co–N=92.6(1)°) in $[Ni\{Co(aet)_3\}_2]^{2+}$, respectively. The bond distances associated with the aet ligands (average S–C=1.823(5) Å, C–C=1.510(6) Å, C–N=1.482(7) Å, N–H=0.87(6) Å, and C–H=0.95(5) Å) are in good agreement with those observed in $[Ni\{Co(aet)_3\}_2]^{2+}$ (average S–C=1.819(5) Å, C–C=1.514(6) Å, and C–N=1.496(7) Å). However, it is noted that the Ni–S distances (average 2.430(1) Å) in **1** are longer than the Ni–S ones (average 2.400(1) Å) in $[Ni\{Co(aet)_3\}_2]^{2+}$, which suggests that the sulfur atoms of the *fac*(*S*)-[Rh(aet)$_3$] unit bind to the central nickel atom more weakly than do the sulfur atoms of the *fac*(*S*)-[Co(aet)$_3$] unit. The average Rh–N distance (2.121(4) Å) in **1** is about 0.12 Å longer than the Co–N one (2.005(4) Å) in $[Ni\{Co(aet)_3\}_2]^{2+}$, as expected from the difference in covalent radii between rhodium and cobalt atoms. On the other hand, the average Rh–S bond distance (2.323(1) Å) is only about 0.07 Å longer than the corresponding Co–S one (average 2.253(1) Å) in $[Ni\{Co(aet)_3\}_2]^{2+}$. These facts suggest that the Rh–S bonds in the *fac*(*S*)-[Rh(aet)$_3$] unit are stronger than the Co–S bonds in the *fac*(*S*)-[Co(aet)$_3$] unit. Accordingly, it is considered that in $[Ni\{Rh(aet)_3\}_2]^{2+}$ (**1**) each thiolato sulfur atom strongly binds to the terminal rhodium atom, which results in the weaker binding to the central nickel atom. A similar trend has been observed in the crystal structure of $[Co\{Ir(aet)_3\}_2]^{3+}$, in which the sulfur atoms of the *fac*(*S*)-[Ir(aet)$_3$] unit bind to the central Co^{III} atom more weakly than do the sulfur atoms of the *fac*(*S*)-[Co(aet)$_3$] unit in $[Co\{Co(aet)_3\}_2]^{3+}$ because of the stronger Ir–S bonds.[10]

Considering the absolute configurations (Δ and Λ) of the two *fac*(*S*)-[Rh(aet)$_3$] units, three isomers ($\Delta\Lambda$, $\Delta\Delta$,

Table 2. Selected Bond Distances (Å) and Angles (deg) for **1**

Ni–S1	2.424(1)	Rh1–N1	2.119(4)
Ni–S2	2.442(1)	Rh1–N2	2.117(3)
Ni–S3	2.431(1)	Rh1–N3	2.121(4)
Ni–S4	2.416(1)	Rh2–S4	2.317(1)
Ni–S5	2.4552(9)	Rh2–S5	2.327(1)
Ni–S6	2.410(1)	Rh2–S6	2.3173(9)
Rh1–S1	2.325(1)	Rh2–N4	2.136(3)
Rh1–S2	2.326(1)	Rh2–N5	2.116(4)
Rh1–S3	2.3273(9)	Rh2–N6	2.115(4)
S1–Ni–S2	83.12(3)	S3–Rh1–N2	174.3(1)
S1–Ni–S3	83.80(4)	S3–Rh1–N3	85.38(8)
S1–Ni–S4	173.01(4)	N1–Rh1–N2	94.5(1)
S1–Ni–S5	102.53(4)	N1–Rh1–N3	95.0(2)
S1–Ni–S6	94.91(4)	N2–Rh1–N3	94.5(1)
S2–Ni–S3	83.30(4)	S4–Rh2–S5	89.08(4)
S2–Ni–S4	90.70(4)	S4–Rh2–S6	87.50(3)
S2–Ni–S5	172.30(5)	S4–Rh2–N4	85.6(1)
S2–Ni–S6	102.66(4)	S4–Rh2–N5	174.9(1)
S3–Ni–S4	98.78(4)	S4–Rh2–N6	89.4(1)
S3–Ni–S5	92.06(4)	S5–Rh2–S6	87.08(4)
S3–Ni–S6	173.73(4)	S5–Rh2–N4	90.9(1)
S4–Ni–S5	83.92(4)	S5–Rh2–N5	85.9(1)
S4–Ni–S6	83.22(4)	S5–Rh2–N6	172.90(8)
S5–Ni–S6	82.22(4)	S6–Rh2–N4	172.9(1)
S1–Rh1–S2	87.93(4)	S6–Rh2–N5	91.36(9)
S1–Rh1–S3	88.35(3)	S6–Rh2–N6	85.92(9)
S1–Rh1–N1	85.9(1)	N4–Rh2–N5	95.3(1)
S1–Rh1–N2	91.6(1)	N4–Rh2–N6	95.9(1)
S1–Rh1–N3	173.69(8)	N5–Rh2–N6	95.5(1)
S2–Rh1–S3	88.24(3)	Ni–S1–Rh1	76.54(4)
S2–Rh1–N1	173.8(1)	Ni–S2–Rh1	76.16(3)
S2–Rh1–N2	86.1(1)	Ni–S3–Rh1	76.36(3)
S2–Rh1–N3	91.1(1)	Ni–S4–Rh2	77.02(4)
S3–Rh1–N1	91.16(9)	Ni–S5–Rh2	76.06(3)
		Ni–S6–Rh2	77.13(3)

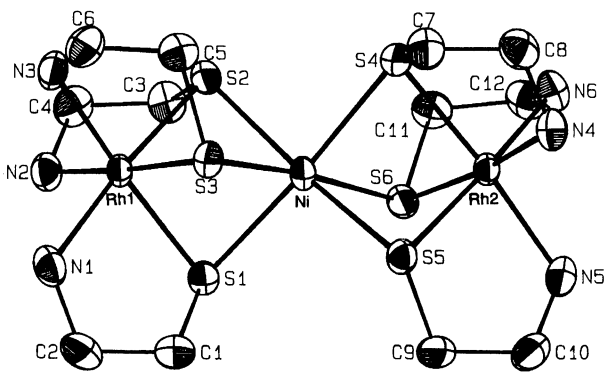

Fig. 1. Perspective view of $[Ni\{Rh(aet)_3\}_2]^{2+}$ (**1**) with the atomic labeling scheme.

and $\Lambda\Lambda$) are possible for $[Ni\{Rh(aet)_3\}_2]^{2+}$. Crystal **1** consists of the $\Delta\Delta$ and $\Lambda\Lambda$ isomers, which combine to form the racemic compound (Fig. 1). All the aet chelate rings have a distinct gauche form with the λ conformation for the $\Delta\Delta$ isomer and the δ conformation for the $\Lambda\Lambda$ one, and therefore all the bridging sulfur atoms are fixed to the *R* configuration for the $\Delta\Delta$ isomer and the *S* configuration for the $\Lambda\Lambda$ one. This stereochemical behavior is wholly consistent with that observed in $[Ni\{Co(aet)_3\}_2]^{2+}$.[15]

Synthesis and Characterization. The reaction of *fac*(*S*)-$[Rh(aet)_3]$ with Ni^{2+} in water at room temperature readily gave a linear-type S-bridged trinuclear complex, $[Ni\{Rh(aet)_3\}_2]^{2+}$ (**1**). The optically active isomers, $(+)^{CD}_{420}$-**1** and $(-)^{CD}_{420}$-**1**, were prepared by the treatment of the optically active T-cage-type S-bridged $Rh^{III}{}_4Zn^{II}{}_3$ complex, $[\{Rh(aet)_3\}_4Zn_3(HO)]^{5+}$,[19] with excess Ni^{2+}. Since $(+)^{CD}_{420}$-**1** and $(-)^{CD}_{420}$-**1**, which were derived from $\Delta\Delta\Delta\Delta$- and $\Lambda\Lambda\Lambda\Lambda$-$[\{Rh(aet)_3\}_4Zn_3(HO)]^{5+}$ respectively, show CD spectra enantiomeric to each other, it is reasonable to assign that the $(+)^{CD}_{420}$ and $(-)^{CD}_{420}$ isomers take the $\Delta\Delta$ and $\Lambda\Lambda$ configurations, respectively. That is, the conversion of the T-cage-type $[\{Rh(aet)_3\}_4Zn_3(HO)]^{5+}$ complex to the linear-type $[Ni\{Rh(aet)_3\}_2]^{2+}$ complex proceeds with retention of the absolute configuration of the *fac*(*S*)-$[Rh(aet)_3]$ unit, as has been observed for the conversion of $[\{Rh(aet)_3\}_4Zn_3(HO)]^{5+}$ to $[Co\{Rh(aet)_3\}_2]^{3+}$.[19] The solid state absorption spectra (KBr disk) of $\Delta\Delta$- or $\Lambda\Lambda$-$\mathbf{1}(NO_3)_2$ and $\mathbf{1}X_2$ (X=Cl, Br, NO_3) agree with each other. This implies that all the complex salts isolated for **1** are the racemic isomer, which is consistent with the crystal structure of $\mathbf{1}(NO_3)_2$.

A similar reaction of Δ_{LLL}-*fac*(*S*)-$[Rh(L\text{-cys-}N,S)_3]^{3-}$ with Ni^{2+} in water produced **2**, which shows a positive CD value at 420 nm. As shown in Fig. 2 and Table 3, the absorption and CD spectra of $(+)^{CD}_{420}$-**2** are quite similar to those of the $(+)^{CD}_{420}$-$\Delta\Delta$ isomer of **1** over the whole region. This clearly indicates that $(+)^{CD}_{420}$-**2** is the linear-type S-bridged $Rh^{III}Ni^{II}Rh^{III}$ complex having the $\Delta_{LLL}\Delta_{LLL}$ configuration, $\Delta_{LLL}\Delta_{LLL}$-$[Ni\{Rh(L\text{-cys-}N,S)_3\}_2]^{4-}$. The reaction solution of Δ_{LLL}-*fac*(*S*)-$[Rh(L\text{-cys-}N,S)_3]^{3-}$ and Ni^{2+} showed the same absorption and CD spectra as those of isolated $(+)^{CD}_{420}$-**2**. Thus, the $\Delta_{LLL}\Delta_{LLL}$ isomer is selectively formed for **2**, retaining the Δ_{LLL} configuration of the starting *fac*(*S*)-$[Rh(L\text{-cys-}N,S)_3]^{3-}$. The selective formation of the $\Delta_{LLL}\Delta_{LLL}$ isomer has also been recognized for $[Co\{Rh(L\text{-cys-}N,S)_3\}_2]^{3-}$, when Δ_{LLL}-*fac*(*S*)-$[Rh(L\text{-cys-}N,S)_3]^{3-}$ was reacted with $[CoCl(NH_3)_5]^{2+}$.[9]

Absorption and CD Spectra. As illustrated in Fig. 2, the absorption spectra of the $Rh^{III}Ni^{II}Rh^{III}$ trinuclear complexes (**1** and **2**) are characterized by two intense bands (about 20 and 24×10^3 cm^{-1}) in the visible region, accompanied by more intense bands in the UV region. Considering that *fac*(*S*)-$[Rh(aet \text{ or } L\text{-cys-}N,S)_3]^{0 \text{ or } 3-}$ had little absorption in the energy region lower than about 24×10^3 cm^{-1} (Fig. 3),[9] the visible absorption bands of **1** and **2** can be assigned as arising from the central $Ni^{II}S_6$ chromophore. Similar intense visible bands have been observed in the absorption spectra of the corresponding $Rh^{III}Co^{III}Rh^{III}$ complexes, $[Co\{Rh(aet \text{ or } L\text{-cys-}N,S)_3\}_2]^{3+ \text{ or } 3-}$ (Fig. 3),

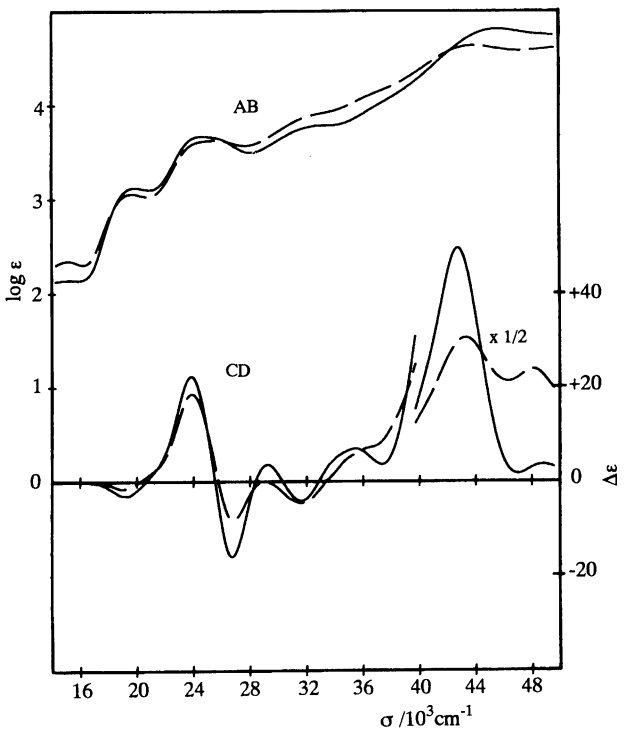

Fig. 2. Electronic absorption and CD spectra of $\Delta\Delta$-$[Ni\{Rh(aet)_3\}_2]^{2+}$ ($\Delta\Delta$-**1**) (—) and $\Delta_{LLL}\Delta_{LLL}$-$[Ni\{Rh(L\text{-cys-}N,S)_3\}_2]^{4-}$ ($\Delta_{LLL}\Delta_{LLL}$-**2**) (— —) in water.

Table 3. Absorption and CD Spectral Data of Complexes in Water

Complex	Absorption maxima $\sigma/10^3$ cm^{-1} ($\log\varepsilon/mol^{-1}\,dm^3\,cm^{-1}$)	CD extrema $\sigma/10^3$ cm^{-1} ($\Delta\varepsilon/mol^{-1}\,dm^3\,cm^{-1}$)
$\Delta\Delta$-$[Ni\{Rh(aet)_3\}_2]^{2+}$		
	19.88 (3.12)	19.34 (−2.98)
	24.63 (3.67)	23.87 (+22.34)
	34.6 (3.8 sh)	26.74 (−15.89)
	45.45 (4.81)	29.24 (+3.58)
		31.55 (−4.01)
		35.46 (+6.94)
		42.74 (+99.3)
		48.78 (+7.3)
$\Delta_{LLL}\Delta_{LLL}$-$[Ni\{Rh(L\text{-cys-}N,S)_3\}_2]^{4-}$		
	19.65 (3.05)	18.98 (−1.56)
	25.58 (3.62)	23.87 (+18.52)
	34.3 (4.0 sh)	26.81 (−8.16)
	43.86 (4.63)	31.55 (−4.52)
		37.2 (+8.1 sh)
		43.3 (+61.2)
		48.1 (+47.8)

The sh label denotes a shoulder.

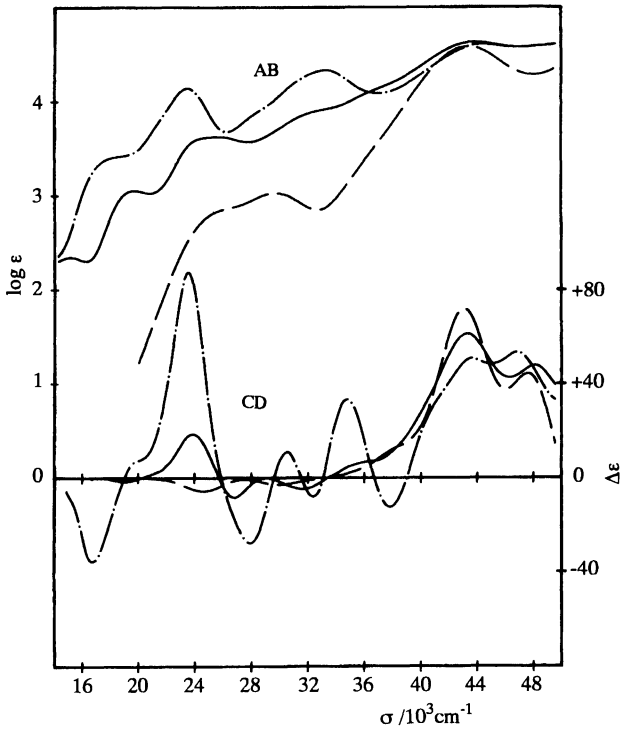

Fig. 3. Electronic absorption and CD spectra of $\Delta_{LLL}\Delta_{LLL}$-$[Ni\{Rh(L\text{-}cys\text{-}N,S)_3\}_2]^{4-}$ ($\Delta_{LLL}\Delta_{LLL}$-**2**) (—), $\Delta_{LLL}\Delta_{LLL}$-$[Co\{Rh(L\text{-}cys\text{-}N,S)_3\}_2]^{3-}$ (---), and Δ_{LLL}-*fac*(*S*)-$[Rh(L\text{-}cys\text{-}N,S)_3]^{3-}$ (— —) in water.

which have been attributed to the central $Co^{III}S_6$ chromophore.[9] The extinction coefficients of these visible bands due to the $Ni^{II}S_6$ and $Co^{III}S_6$ chromophores are commonly greater than 10^3 $mol^{-1}\,dm^3\,cm^{-1}$, suggesting that these bands are dominated by the sulfur-to-metal (Ni^{II} or Co^{III}) change transfer (SMCT) transitions. This assignment is compatible with the similarity of the visible bands between the $Rh^{III}Ni^{II}Rh^{III}$ and $Rh^{III}Co^{III}Rh^{III}$ complexes, considering that the SMCT transition terminates on a e_g orbital for both the octahedral Ni^{II} and Co^{III}. It is noticed that the visible bands due to the $Ni^{II}S_6$ chromophore for **1** and **2** are at the higher energy side with lower intensities, compared with the visible bands due to the $Co^{III}S_6$ chromophore for $[Co\{Rh(aet \text{ or } L\text{-}cys\text{-}N,S)_3\}_2]^{3+ \text{ or } 3-}$. This is to be expected for the SMCT transitions since the divalent Ni^{II} is a poorer oxidant that is the trivalent Co^{III}. In the CD spectrum, $\Delta\Delta$-**1** and $\Delta_{LLL}\Delta_{LLL}$-**2** exhibit major positive and negative CD bands (ca. 24 and 27×10^3 cm^{-1}, respectively) from lower energy in the visible region (Fig. 2). The same CD spectral pattern has been observed for the $\Delta\Delta$-type isomers of $[Co\{Rh(aet \text{ or } L\text{-}cys\text{-}N,S)_3\}_2]^{3+ \text{ or } 3-}$ in the same region (Fig. 3).[9] This seems to reflect the fact that all the asymmetric sulfur atoms of the $\Delta\Delta$-type $Rh^{III}Ni^{II}Rh^{III}$ isomers have the *R* configuration as do the sulfur atoms of the $\Delta\Delta$-type $Rh^{III}Co^{III}Rh^{III}$ isomers. However, the CD intensities for these $Rh^{III}Ni^{II}Rh^{III}$ complexes are much lower than those for the corresponding $Rh^{III}Co^{III}Rh^{III}$ complexes, in parallel with the absorption spectral behavior.

The most intense band (about 44×10^3 cm^{-1}) in the UV region for **1** and **2** corresponds well to the sulfur-to-rhodium charge transfer band observed for the mononuclear *fac*(*S*)-$[Rh(aet \text{ or } L\text{-}cys\text{-}N,S)_3]^{0 \text{ or } 3-}$ complexes (Fig. 3).[9] Moreover, in this region the CD spectrum of $\Delta_{LLL}\Delta_{LLL}$-**2** is very similar to that of Δ_{LLL}-*fac*(*S*)-$[Rh(L\text{-}cys\text{-}N,S)_3]^{3-}$, giving two positive CD bands at 43.25 and 48.08×10^3 cm^{-1}. Similar absorption and CD spectral correlations have been recognized between $[Co\{Rh(aet \text{ or } L\text{-}cys\text{-}N,S)_3\}_2]^{3+ \text{ or } 3-}$ and *fac*(*S*)-$[Rh(aet \text{ or } L\text{-}cys\text{-}N,S)_3]^{3-}$ (Fig. 3).[9] From these facts, it is seen that the absorption and CD spectra of the linear-type $Rh^{III}MRh^{III}$ trinuclear complexes at around 45×10^3 cm^{-1} are dominated by the terminal *fac*(*S*)-$[Rh(aet \text{ or } L\text{-}cys\text{-}N,S)_3]^{0 \text{ or } 3-}$ units having a $Rh^{III}N_3S_3$ chromophore.

Properties. The absorption spectrum of $\Delta\Delta$-**1** or $\Lambda\Lambda$-**1** in methanol is essentially the same as that in solid state (KBr disk). Furthermore, no significant absorption and CD spectral changes with time were recognized for $\Delta\Delta$-**1** or $\Lambda\Lambda$-**1** in methanol at room temperature for several hours. These facts point out that not only the S-bridged $Rh^{III}Ni^{II}Rh^{III}$ trinuclear structure but also the chiral configuration around the *fac*(*S*)-$[Rh(aet)_3]$ unit are retained in methanol. However, a 1 : 1 mixture of $\Delta\Delta$-**1** and $\Lambda\Lambda$-**1** in methanol was found to have an absorption spectral change with time under the same conditions. As shown in Fig. 4, the absorption spectrum changes from Curve 1 (t=0) to Curve 4 (t=4 h), having the well-defined isosbestic points at 331, 355, 376, and 419 nm. It has been shown that the $\Delta\Lambda$ (*meso*) isomer gives an absorption curve deviated from that of the $\Delta\Delta/\Lambda\Lambda$ isomer for the linear-type S-bridged $MCo^{III}M$ complexes, $[Co\{M(aet)_3\}_2]^{3+}$

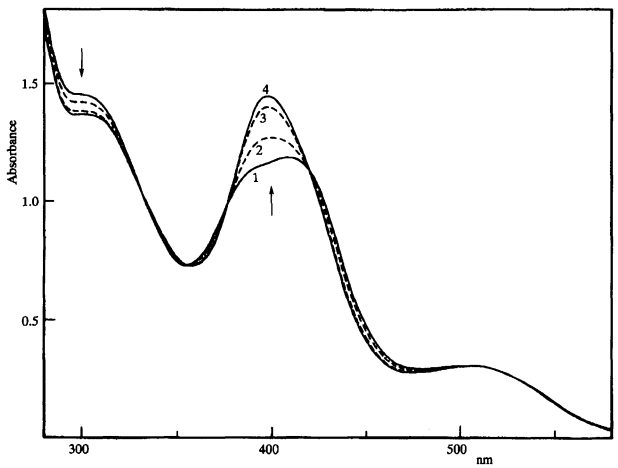

Fig. 4. Absorption spectral change with time for a 1 : 1 mixture of $\Delta\Delta$-**1** and $\Lambda\Lambda$-**1** in methanol (2.6×10^{-4} mol dm^{-3}) at 23 °C; Curves 1—4 were measured at 0, 30, 120, 240 min, respectively.

(M=Co^{III}, Rh^{III}, Ir^{III}).[7,9,10] Furthermore, the conversion of racemi- to *meso*-$[Co\{Ir(aet)_3\}_2]^{3+}$ has undergone a similar absorption spectral change.[10] Accordingly, it is reasonable to consider that this absorption spectral change is caused by the formation of the $\Delta\Lambda$ isomer in solution, which results from the intermolecular exchange of the Δ- or Λ-*fac*(*S*)-$[Rh(aet)_3]$ units but not from the racemization of the Δ- or Λ-*fac*(*S*)-$[Rh(aet)_3]$ unit. The standard first-order kinetic plots of $\ln(A_t - A_\infty)$ vs. t (at 398 nm) are linear for more than three half-lives, and from these plots the first-order rate constant (K_{obsd}) was evaluated to be 2.65×10^{-4} s^{-1} ($t_{1/2}$=44 min). As expected, the same absorption spectral change was noticed for **1** in methanol, which exists as the racemic isomer in solid state. Considering that the absorption spectral change with time for the racemic isomer of $[Ni\{Co(aet)_3\}_2]^{2+}$ in methanol is negligibly small under the same conditions, it is assumed that the Ni–S bonds in **1** are weaker than those in $[Ni\{Co(aet)_3\}_2]^{2+}$, which is compatible with the X-ray analytical result.

The absorption and CD spectra of $\Delta\Delta$-**1** or $\Lambda\Lambda$-**1** in water at t=0 coincide well with those observed in methanol, although their intensities slightly decreases with time (about 5% absorption and CD decreases for 1 h at 404 and 419 nm, respectively). On the other hand, the absorption spectrum of **1** or a 1 : 1 mixture of $\Delta\Delta$-**1** and $\Lambda\Lambda$-**1** in water at t=0 has Curve 4, which is observed in methanol at t=4 h. This spectral behavior implies that in water the intermolecular exchange of the *fac*(*S*)-$[Rh(aet)_3]$ units occurs instantaneously to afford the $\Delta\Lambda$ isomer. Since the reaction solution of *fac*(*S*)-$[Rh(aet)_3]$ and Ni^{2+} in water showed an absorption curve quite similar to Curve 4, it is probable that both the meso ($\Delta\Lambda$) and racemic ($\Delta\Delta/\Lambda\Lambda$) isomers are formed in solution for **1**, as in the case of $[Co\{Rh(aet)_3\}_2]^{3+}$.[9] However, attempts to isolate the meso isomer by fractional crystallization were unsuccessful. This can be ascribed to the greater solubility of the *meso* isomer and the rapid intermolecular exchange of the *fac*(*S*)-$[Rh(aet)_3]$ units. In addition, separation of the *meso* and racemic isomers was not achieved by the SP-Sephadex column chromatography because of complete decomposition in the column. These chemical properties of **1** differ significantly from those observed for $[Co\{Rh(aet)_3\}_2]^{3+}$, in which the *meso* and racemic isomers have easily been separated and isolated by the fractional crystallization or the column chromatographic technique owing to the high stability in solution.[9]

References

1) D. H. Busch and D. C. Jicha, *Inorg. Chem.*, **1**, 884 (1962).

2) G. R. Brubaker and B. E. Douglas, *Inorg. Chem.*, **6**, 1562 (1967).

3) M. J. Heeg, E. L. Blinn, and E. Deutsch, *Inorg. Chem.*, **24**, 1118 (1985).

4) T. Konno, S. Aizawa, K. Okamoto, and J. Hidaka, *Chem. Lett.*, **1985**, 1017.

5) K. Okamoto, S. Aizawa, T. Konno, H. Einaga, and J. Hidaka, *Bull. Chem. Soc. Jpn.*, **59**, 3859 (1986).

6) S. Aizawa, K. Okamoto, H. Einaga, and J. Hidaka, *Bull. Chem. Soc. Jpn.*, **61**, 1601 (1988).

7) S. Miyanowaki, T. Konno, K. Okamoto, and J. Hidaka, *Bull. Chem. Soc. Jpn.*, **61**, 2987 (1988).

8) T. Konno, S. Aizawa, and J. Hidaka, *Bull. Chem. Soc. Jpn.*, **62**, 585 (1989).

9) T. Konno, S. Aizawa, K. Okamoto, and J. Hidaka, *Bull. Chem. Soc. Jpn.*, **63**, 792 (1990).

10) T. Konno, K. Nakamura, K. Okamoto, and J. Hidaka, *Bull. Chem. Soc. Jpn.*, **66**, 2582 (1993).

11) R. E. DeSimone, T. Ontko, L. Wardman, and E. L. Blinn, *Inorg. Chem.*, **14**, 1313 (1975).

12) E. L. Blinn, P. Butlar, K. M. Chapman, and S. Harris, *Inorg. Chim. Acta*, **24**, 139 (1977).

13) D. W. Johnson and T. R. Brewer, *Inorg. Chim. Acta*, **151**, 221 (1988).

14) T. Konno, K. Okamoto, and J. Hidaka, *Bull. Chem. Soc. Jpn.*, **63**, 3027 (1990).

15) T. Konno, K. Okamoto, and J. Hidaka, *Acta Crystallogr., Sect. C*, **49**, 222, (1993).

16) T. Konno, K. Okamoto, and J. Hidaka, *Chem. Lett.*, **1990**, 1043.

17) T. Konno, K. Okamoto, and J. Hidaka, *Inorg. Chem.*, **30**, 2253 (1991).

18) T. Konno, T. Nagashio, K. Okamoto, and J. Hidaka, *Inorg. Chem.*, **31**, 1160 (1992).

19) T. Konno, K. Okamoto, and J. Hidaka, *Bull. Chem. Soc. Jpn.*, **67**, 101 (1994).

20) T. Konno, K. Okamoto, and J. Hidaka, *Inorg. Chem.*, **33**, 538 (1994).

21) K. Okamoto, T. Konno, and J. Hidaka, *J. Chem. Soc., Dalton Trans.*, **1994**, 533.

22) K. Okamoto, T. Konno, Y. Kageyama, and J. Hidaka, *Chem. Lett.*, **1992**, 1105.

23) T. Konno, K. Okamoto, and J. Hidaka, *Inorg. Chem.*, **31**, 3875 (1992).

24) T. Konno, K. Kageyama, and K. Okamoto, *Bull. Chem. Soc. Jpn.*, **67**, 1957 (1994).

25) M. Kita, K. Yamanari, and Y. Shimura, *Bull. Chem. Soc. Jpn.*, **56**, 3272 (1983).

26) C. K. Fair, MOLEN, "Interactive Structure Solution Procedure," Enraf-Nonius, Delft, The Netherlands (1990).

27) Lists of structure factors, complete bond distances and angles, anisotropic thermal parameters, and hydrogen atom coordinates are deposited as Document No. 68002 at the Office of the Editor of Bull. Chem. Soc. Jpn.